

FF

ISTITUTO NAZIONALE DI FISICA NUCLEARE

Sezione di Trieste

INFN/TC-94/13

7 settembre 1994

SW 2475

F. Arfelli, G. Barbiellini, S. Bernstorff, A. Bravin, G. Cantatore, E. Castelli,
L. Dalla Palma, M. Di Michiel, R. Longo, P. Poropat, R. Rosei, A. Savoia, M. Sessa,
G. Tromba, and A. Vacchi

DIGITAL MAMMOGRAPHY WITH SYNCHROTRON RADIATION

SCAN-9411024



CERN LIBRARIES, GENEVA

DIGITAL MAMMOGRAPHY WITH SYNCHROTRON RADIATION

*F. Arfelli, A. Bravin, G. Barbiellini, G. Cantatore, E. Castelli,
M. Di Michiel, P. Poropat, R. Rosei, M. Sessa and A. Vacchi*

Dipartimento di Fisica dell' Università di Trieste, Italy

and

Sezione INFN di Trieste, Italy

S. Bernstorff, R. Rosei, A. Savoia and G. Tromba

Società Sincrotrone Trieste, Italy

L. Dalla Palma and R. Longo,

Istituto di Radiologia dell' Università di Trieste and USL Trieste, Italy

Presented to the:

FIFTH INTERNATIONAL CONFERENCE

ON SYNCHROTRON RADIATION INSTRUMENTATION

18-22 July 1994, Stony Brooks, NY - USA

Abstract

The SYRMEP (SYnchrotron Radiation in MEDical Physics) Collaboration is planning to use a beam of monochromatic X-rays provided by Elettra, the synchrotron radiation facility in operation at Trieste (Italy), in conjunction with a novel silicon pixel detector to conduct research in digital mammography.

A beamline dedicated to mammography is presently under construction in Trieste; it will provide, at a distance of about 20 m from an Elettra bending magnet, a monochromatic laminar-section ($150 \times 4 \text{ mm}^2$) X-ray beam. This beam will illuminate in vitro samples and will be detected by a fixed silicon microstrip device forming a matrix of pixels. Digital images of phantoms having a size common in the diagnostic practice ($150 \times 150 \text{ mm}^2$), can then be produced by scanning the sample itself in front of the detector. A prototype detector with a sensitive area of $24 \times 1 \text{ mm}^2$ and pixels of $0.5 \times 0.5 \text{ mm}^2$ has been built and tested. We present the current status of the SYRMEP beamline and a digital image of a mammographic phantom exposed to a radioactive X-ray source.

Introduction

A considerable interest has been generated by digital radiology as a possible technique to obtain high quality diagnostic images amenable to computer enhancement techniques, while reducing the overall radiation dose delivered to the patient. Furthermore, in the case of mammography for instance, a monochromatic source of X-rays will improve the quality of the images, with special regard to contrast resolution (see Ref. 1 and 2).

The SYRMEP collaboration is developing a project to conduct research in digital mammography using a synchrotron radiation monochromatic X-ray beam as the illuminating source, and a silicon pixel detector to collect the photons transmitted by the sample. Figure 1 shows a conceptual scheme of the beamline of the SYRMEP project. An X-ray beam provided by a bending magnet from Elettra, the synchrotron light source now in operation in Trieste, Italy, is passed through a slit and a monochromator system and then used to illuminate a sample.

Digital images are produced by scanning the sample through the beam-detector assembly and by counting each single photon impinging on a detector pixel. The number of photons is then mapped into a shade of grey or into a color hue.

The combination of a monochromatic laminar beam with a very high efficiency laminar detector allows one to minimize the radiation dose delivered to the sample. Matching a laminar-section beam with a laminar detector strongly reduces unwanted detection of scattered radiation, making it therefore possible to eliminate the need for an anti-scatter grid [3].

The ability to count single photons means that the SYRMEP detector will yield the highest possible contrast resolution, while the fact that the data are in digital form will allow enhancement techniques to be applied to the images [4,5].

In the following we will discuss in some detail the SYRMEP beamline, which is at present under construction at Elettra. A sample image will be shown after a brief description of the detector, followed by a short discussion of the future perspectives of the SYRMEP project.

The SYRMEP beamline

The source of radiation used by the SYRMEP beamline is one of the 24 bending magnets of the Elettra ring. The beam has an angular vertical intensity distribution which is Gaussian with a standard deviation given in Table I below as function of the emitted

radiation energy. Table values are calculated for the Elettra design parameters, $E_e = 2$ GeV, $I_e = 400$ mA, and $E_C = 3.2$ keV, where E_e is the electron beam energy, I_e is the electron current and E_C is the critical energy [6].

In the horizontal direction the distribution is uniform over the 7 mrad angle which is covered by the SYRMEP beamline light-port. Figure 2 shows a schematic layout of the beamline along with distances calculated from the radiation source. The beamline proper begins at a light-port of the storage ring located at a distance of 2098 mm from the midpoint of the bending magnet, which corresponds to the source position. This hard X-ray line is a controlled-access one and it basically consists of three parts, the front-end hutch, the intermediate hutch and the experimental hutch. The front-end is completely enclosed within the concrete shielding walls of the storage ring. All bending-magnet front-ends operating at Elettra have been standardized [7]. A three-way beam splitter is built in each of the above front-ends. In this way every bending magnet feeds three separate beamlines, each with a horizontal angular aperture of 7 mrad. After the front-end, one finds a Be window which will cut lower energy photons. Beam defining slits are contained in a second chamber downstream, just before the monochromator chamber. A tungsten beam stopper is installed after the monochromator crystal. This will allow access to the experimental area while the beam is on without prejudice to the thermal stability of the crystal. A final Be window before the experimental area will serve as a vacuum-air interface. The experimental hutch, which is located at about 22 m from the bending magnet, will contain a fast shutter, a flux monitor, an imaging slit system, the sample with its movement stages, and the detector with its associated electronics.

The first Be window separates the storage ring vacuum ($\sim 10^{-10}$ Torr) from the beamline vacuum ($\sim 10^{-7}$ Torr). It consists of a 120×12 mm² rectangular Be foil with a thickness of 2 mm. This foil is brazed onto a suitable aperture cut in a water-cooled OFHC copper disk having a diameter of 150 mm and a thickness of 12 mm. The window will also act as a filter cutting lower photon energies and avoiding an excessive heat load on the downstream optics. Figure 3 shows a comparison between the window transmission spectrum and that of the bending magnet. Incident light power on the window is ~ 113 W while transmitted power is ~ 25 W. This yields a temperature gradient between the center of the Be window and its edges of ~ 6 °C [8], which can be easily handled by our simple cooling scheme.

The cross-section of the beam impinging on the monochromator crystal is defined by a set of two orthogonal water-cooled copper slit systems. Slit blades are moved by stepping motors and can achieve a 1 μ m positioning accuracy. In the running condition this cross section is $\sim 110 \times 3$ mm². At the detector position the beam cross section will be

about 150x4 mm². Slit blades will be coated with a photoluminescent film allowing a rough visual monitoring of the beam position.

A schematic perspective view of the monochromator, which will be at a distance of about 18 m from the source, is shown in Figure 4. The crystal itself is a monolithic channel-cut Si(1,1,1). Since there is a trade-off between transmitted flux and energy resolution the Si(1,1,1) appears to be a suitable choice for our beamline. Figure 5 shows the rocking-curve for a Si(1,1,1) crystal [9]. It can be seen that the FWHM at 20 keV is 0.013 mrad. This would correspond, with an incident parallel beam, to an energy resolution of 10⁻⁴; the natural vertical divergence of the beam degrades the energy resolution to about 10⁻³, which is however still sufficient for our imaging purposes. With the given dimensions, the crystal will be able to accept the entire beam cross-section at its position. The dispersion plane is vertical, while the rotation axis of the crystal is orthogonal to the diffraction plane and passes through the midpoint of the first surface. The whole assembly can be rotated by means of a stepping motor with an angular resolution of 0.010 mrad through a range of Bragg angles between 3.24° and 11.40°. This will result in an exit beam energy range between 10 and 35 keV: for all those energies the exit beam will still be parallel to the incident beam, with a separation of ~20 mm. The vertical beam displacement between the maximum and minimum energy positions will only be of about 0.3 mm. The imaging-slit/sample/detector assembly can be easily moved to accommodate for this displacement. Incident light power will be about 25 W, so that the first crystal surface has to be cooled in order to avoid crystal damage caused by excessive heating.

The detector

The SYRMEP detector is a silicon microstrip device used in an innovative geometrical configuration in which radiation impinges on the side rather than on the surface of the chip and is therefore totally absorbed within the active volume of the detector. The pixel dimensions are then defined by the thickness of the silicon chip and by the microstrip pitch. A detailed description of this device can be found in Ref. 10. Figure 6 shows a digital image obtained with the SYRMEP prototype detector. The sample was a detail from a standard mammographic phantom consisting of two 300 µm diameter quartz spheres floating in a 1 mm depth of wax. This detail was embedded in 16 mm thick plexiglas. The sample was illuminated by a 22 keV radioactive point source and the image was obtained by scanning the pixel linear array of the detector in front of the sample with

a sampling step of 100 μm . A superficial dose on the surface of the sample of 360 μGy was necessary to obtain the image [11].

Perspectives

The SYRMEP beamline has been completely specified in its design stage and it is presently being constructed at the Elettra site in Trieste, Italy. We foresee that in about a year from now we will be able to have the first beam and to initiate preliminary tests. In the meantime we are developing a second generation detector along with its associated electronics. This detector will consist of a stack of four Si chips each having 250 $200 \times 300 \mu\text{m}^2$ pixels, and the read-out electronics will be made of custom designed VLSI chips bonded to the detector.

References and notes

- [1] L. Benini et al., Synchrotron Radiation Application to Digital Mammography. A Proposal for the Trieste Project "Elettra", Phys. Med., Vol. VI (1990) p.293.
- [2] E. Burattini et al., X-ray Mammography with Synchrotron Radiation, Rev. of Sci. Instr., Vol. 63, no. 1 (1992), p.638.
- [3] G.T. Barnes, X. Wu, P.C. Sanders, Scanning Slit Chest Radiography: a Practical and Efficient Scatter Control Design, Radiology, Vol. 190 (1994), p.525.
- [4] F. Arfelli et al., SYnchrotron Radiation for MEDical Physics. A Comparison Between Digital and Conventional Screen-Film Images, Phys. Med., Vol. IX (1993) p.175.
- [5] F. Arfelli et al., SYRMEP(SYnchrotron Radiation for MEDical Physics). Performance of the Digital Detection System, Phys. Med., Vol. IX, Suppl. 1 (1993) p.229.
- [6] Elettra Conceptual Design Report, Societa' Sincrotrone Trieste, Trieste (1989).
- [7] Sincrotrone Trieste Scientific Division, Specifications of Bending Magnet Front-Ends, Report no. ST/DS-FE-92/2 (1992).
- [8] R.T. Avery, Thermal Problems on High Flux Beam Lines, Nucl. Instr. and Meth., Vol. 222 (1984), p. 146.
- [9] T. Matsushita, X-ray Monochromators, in Handbook of Synchrotron Radiation, Vol. 1a, E.E. Koch ed., North Holland Publ. Co. (1983), p. 261.
- [10] F. Arfelli et al., Silicon X-ray Detector for Synchrotron Radiation Digital Radiology, I.N.F.N. Report no. INFN/TC-94/09 (1994), to be published in Nucl. Instr. and Methods.
- [11] For a more thorough discussion of the experimental technique and of image processing see for instance M. Di Michiel, Un Rivelatore di Silicio a Pixel per Immagini in Radiologia Diagnostica, Thesis, Università di Trieste (1994), unpublished.

Table I

Standard deviation of the beam vertical angular divergence distribution as a function of emitted radiation energy.

E (keV)	σ_{tot} (mrad)
10	0.090
15	0.076
20	0.069
25	0.063
30	0.059
35	0.056

Figure captions

Figure 1 Conceptual drawing of the SYRMEP beamline.

Figure 2 Beamline layout. The ruler just below the drawing shows distances in mm. Numbers above this ruler identify individual components (see text). No. 1 is the front-end, no. 7 is the first Be window, no. 12 is the double slit system, no. 13 is the monochromator chamber, no. 17 is the beam stopper, and no. 20 is the second Be window. Distances from the source in mm are shown by the bottom ruler.

Figure 3 Transmission spectrum of the 2 mm Be window. The vertical axis gives the number of photons transmitted per unit time within a 1 mrad horizontal angle in 0.1% of the total bandwidth. The dotted curve represents the spectrum in absence of the Be window, while the solid curve shows the transmission spectrum when the window is inserted.

Figure 4 Schematic perspective view of the monochromator crystal (see text). X is the crystal rotation axis, and the ~20 mm separation between the incident and the exit beam, as represented by the arrows, is also shown.

Figure 5 Rocking curve of a channel cut Si(1,1,1) crystal (see text).

Figure 6 Contrast enhanced digital image of a detail from a mammographic phantom (see text). The dark edges of the image are due to photons transmitted through 16 mm of plexiglas. The lighter center area is due to 15 mm of plexiglas and a thickness of about 1 mm of wax. Two 300 μm diameter quartz spheres can be seen within the latter.

THE POLYMERIZATION OF VINYL MONOMERS

The polymerization of vinyl monomers is a process in which the monomers react to form a polymer chain. This reaction is initiated by a free radical, which then propagates the chain by adding more monomers. The rate of polymerization is dependent on the concentration of the monomers and the initiator, as well as the temperature and the presence of inhibitors.

The polymerization of vinyl monomers is a complex process that involves several steps. The first step is the initiation of the reaction, which is typically initiated by a free radical. The second step is the propagation of the chain, where the radical adds to the monomers to form a growing polymer chain. The third step is the termination of the reaction, where the growing chain reacts with another radical to form a stable polymer molecule.

The rate of polymerization is affected by several factors, including the concentration of the monomers and the initiator, the temperature, and the presence of inhibitors. Higher concentrations of monomers and initiator generally lead to a faster rate of polymerization. Higher temperatures also increase the rate, but can also lead to side reactions and the formation of lower molecular weight polymers.

Inhibitors are substances that can interfere with the polymerization process, either by reacting with the free radical or by blocking the active sites on the growing chain. They are often used to control the rate of polymerization and to prevent unwanted side reactions. Common inhibitors include hydroquinone and benzoyl peroxide.

The polymerization of vinyl monomers is a fundamental process in the synthesis of many polymers. Understanding the kinetics and mechanism of this reaction is essential for the design and optimization of polymerization processes. The study of this reaction has led to the development of many new polymer materials and has provided valuable insights into the behavior of free radicals in chemical reactions.

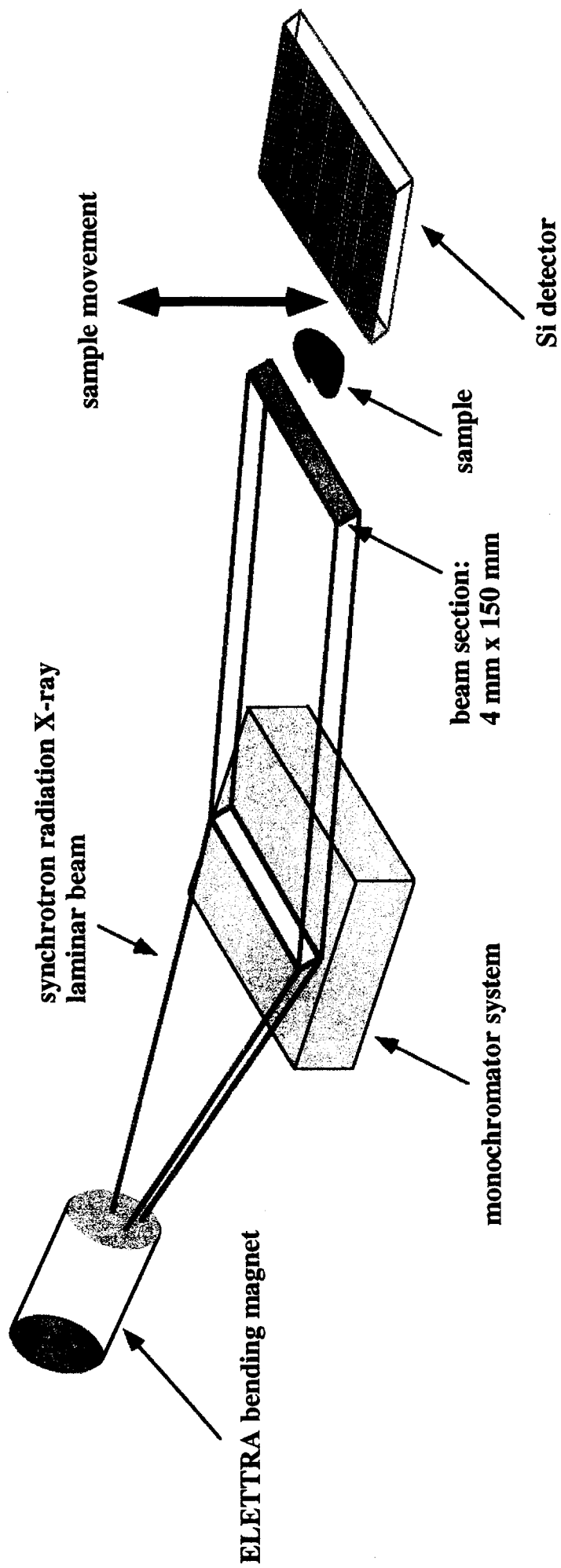


Fig. 1

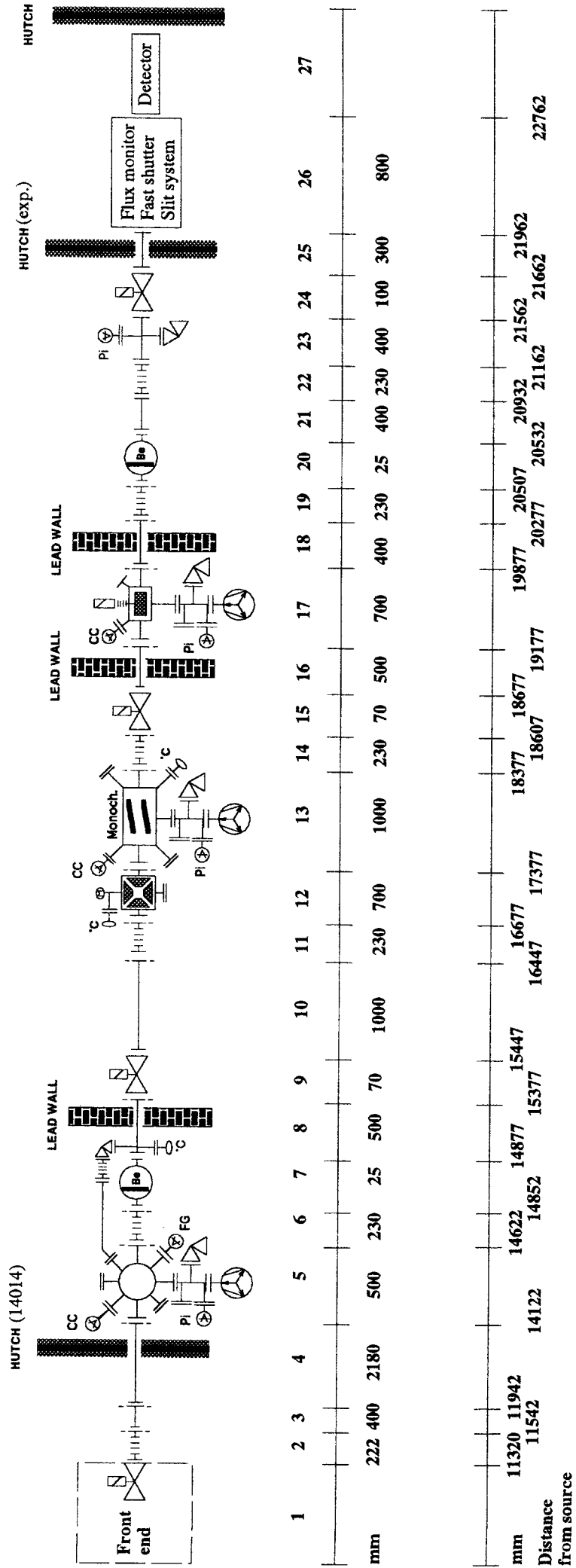


Fig. 2



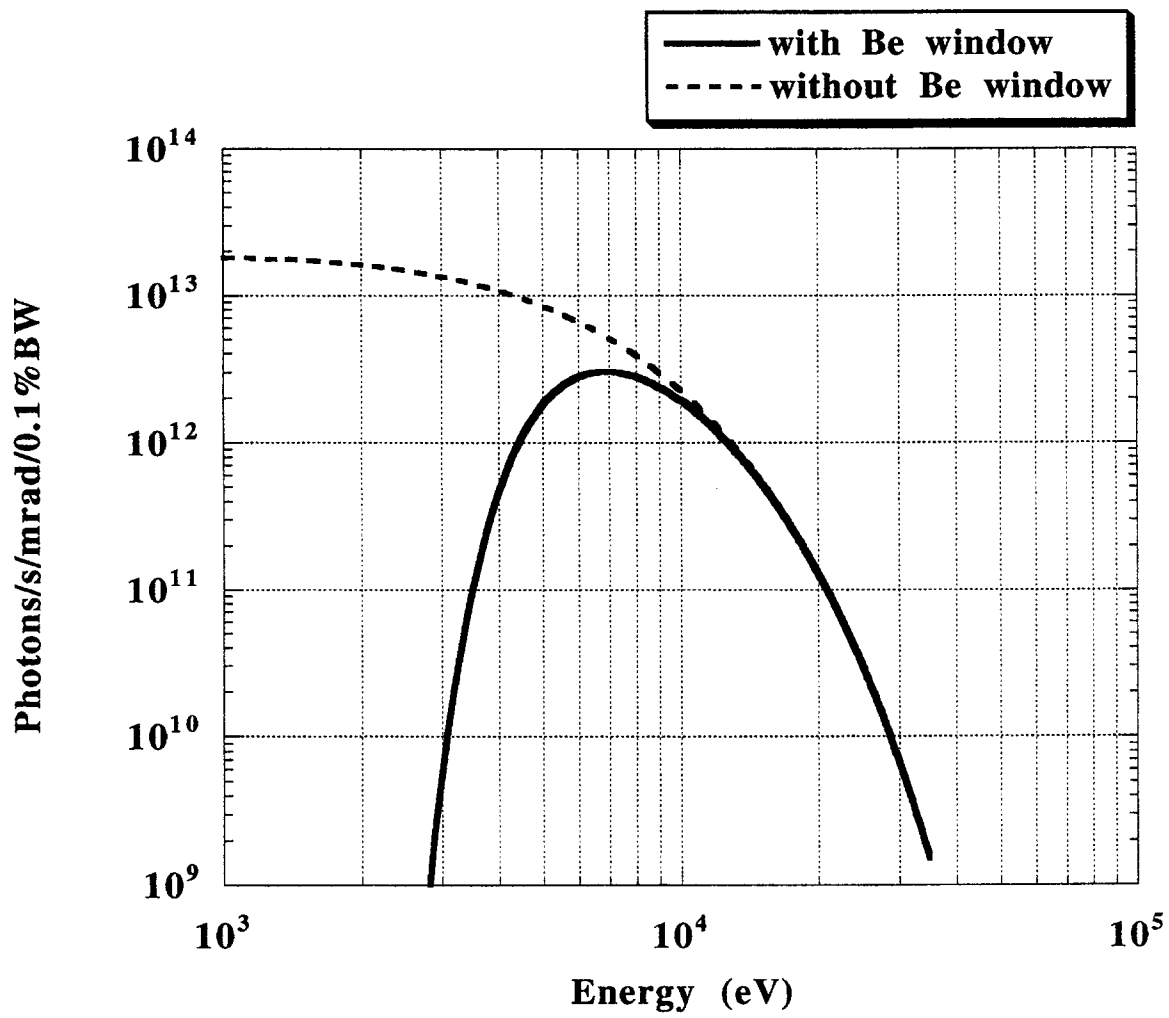
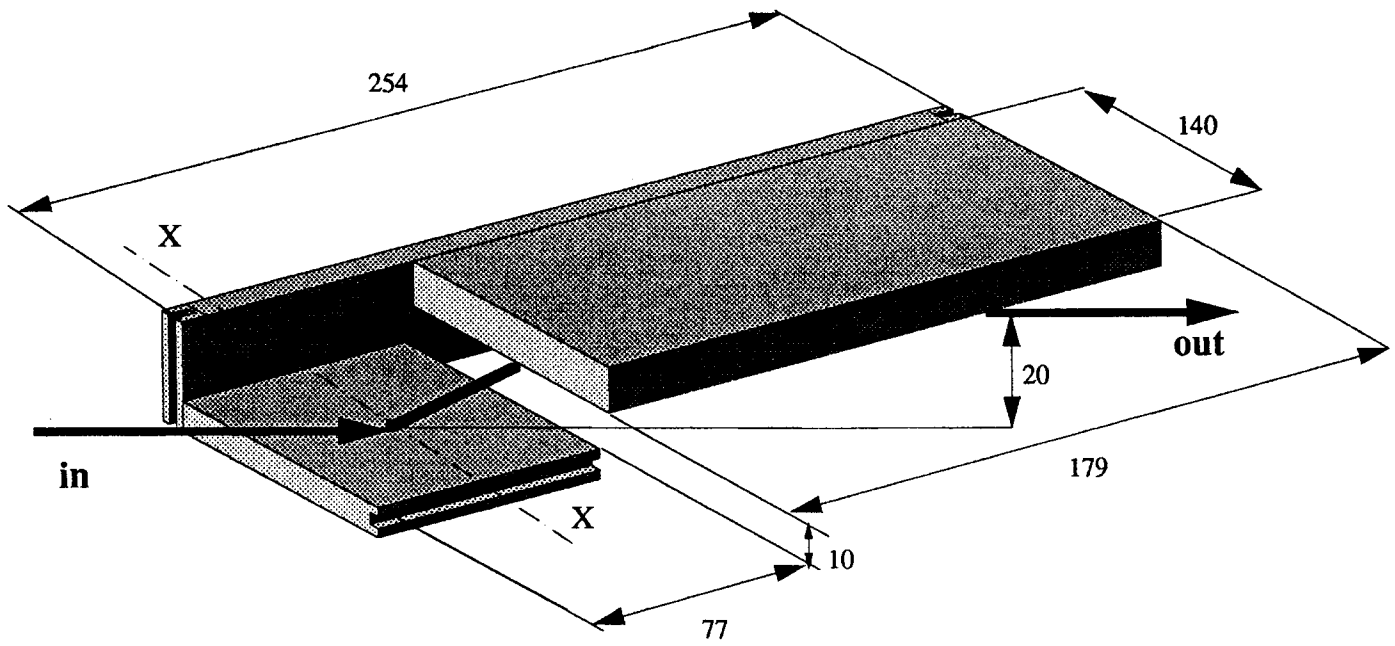


Fig. 3



Dimensions in mm

Fig. 4

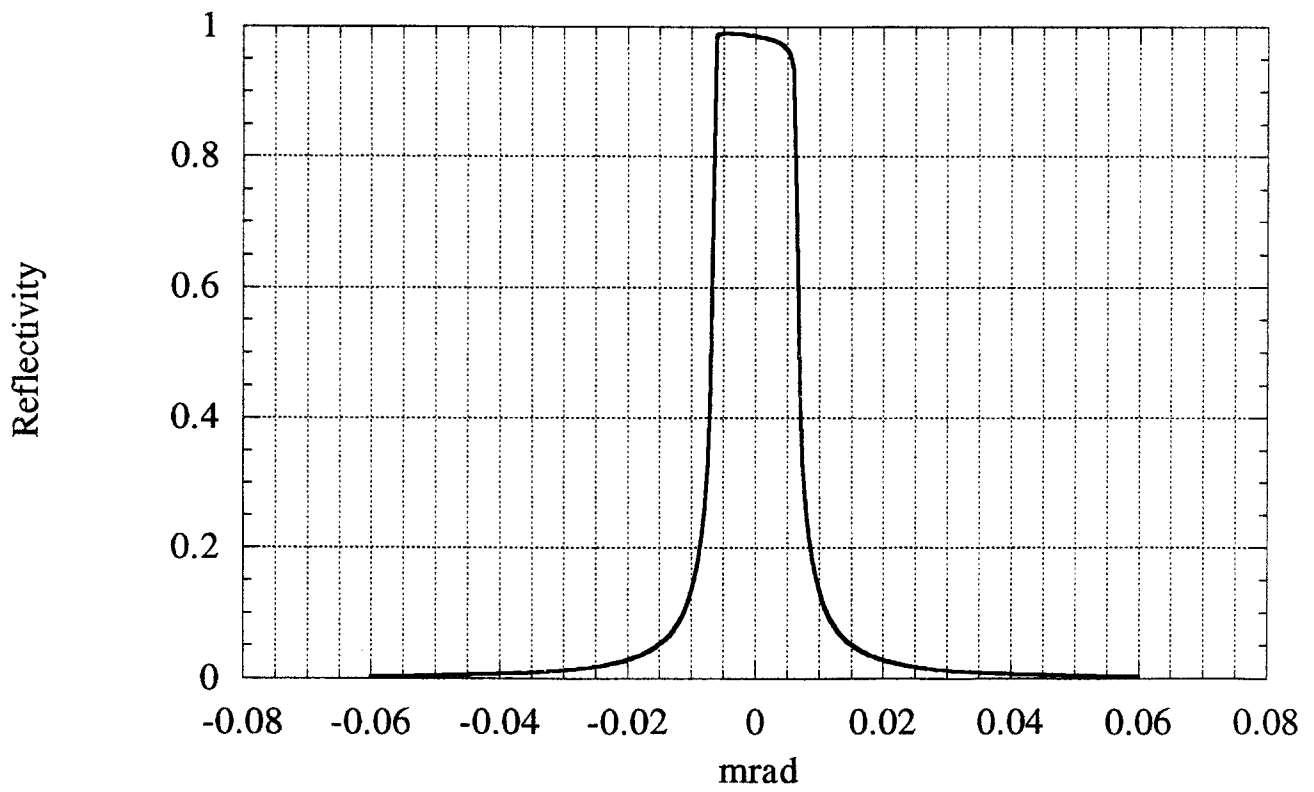


Fig. 5



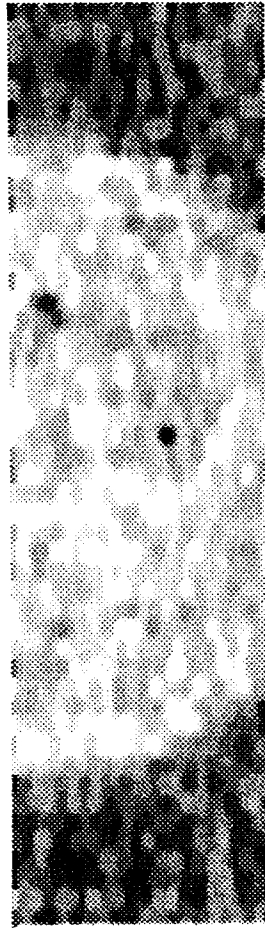


Fig. 6

